Journal of Alloys and Compounds 509 (2011) 2487–2492

Contents lists available at ScienceDirect

Journal of Alloys and Compounds

journal homepage: www.elsevier.com/locate/jallcom

Synthesis and characterization of spinel-type zinc aluminate nanoparticles by a modified sol–gel method using new precursor

Fatemeh Davar[a,**], Masoud Salavati-Niasari[a,b,*]

[a] Institute of Nano Science and Nano Technology, University of Kashan, Kashan, P. O. Box. 87317-51167, I. R. Iran
[b] Department of Inorganic Chemistry, Faculty of Chemistry, University of Kashan, Kashan, P. O. Box. 87317-51167, I. R. Iran

ARTICLE INFO

Article history:
Received 23 June 2010
Received in revised form 3 November 2010
Accepted 10 November 2010
Available online 18 November 2010

Keywords:
Nanoparticles
Sol–gel processes
Inorganic materials

ABSTRACT

In the present paper, we report the successful synthesis of spinel-type of zinc aluminate ($ZnAl_2O_4$) nanoparticles by a modified sol–gel method. Aluminum nitrate and $Zn(en)_2^{+}$ complex (en: ethylenediamine) as new Zn^{2+} source were used. Diethylene glycol monoethyl ether and citric acid are employed as solvent and chelating agent. This method starts from the precursor complex, and involves formation of homogeneous solid intermediates, reducing atomic diffusion paths during thermal treatment. ZnO and $ZnAl_2O_4$ nanocrystals were obtained when the precursor was heat-treated at 350 °C in air for 2 h. The stages of the formation of $ZnAl_2O_4$, as well as the characterization of the resulting compounds were done using thermo-gravimetric analysis (TGA), X-ray diffraction (XRD), scanning electron microscopy (SEM), and Fourier transform infrared spectroscopy (FTIR). The structure, particle size, and temperature of formation of $ZnAl_2O_4$ phases were found to depend on the precursors and methods used for preparation and the calcination temperature. The lowest temperature for preparation of the $ZnAl_2O_4$ is about 550 °C.

1. Introduction

Transition metal-oxide spinels are important in many application fields because of their high thermal resistance and catalytic, electronic and optical properties. They are commonly used in semiconductor and sensor technology as well as in heterogeneous catalysis [1,2]. Among the most interesting materials of that kind, zinc aluminate ($ZnAl_2O_4$), with spinel structure belonging to *Fd*3*m* space group, offers many advantages, such as high thermal and chemical stability, hydrophobic behavior, high mechanical resistance, low sintering temperature, and high quantum yields [3–6]. $ZnAl_2O_4$ is widely used as electronic, ceramic, catalytic material and emerging as one of the best wide band gap compound semiconductor (E_g = 3.8 eV) for various optoelectronic applications [7].

ZnO is one of the most important functional oxides with a direct, wide band gap (3.37 eV) and large excitation binding energy (60 meV), exhibiting many interesting properties including transparent conductivity and piezoelectricity [8–11].

In general, there are many methods of preparation of $ZnAl_2O_4$ such as: solid-state reaction of zinc and aluminium oxides [12,13], co-precipitation method [14], hydrothermal [15,16], microwave-hydrothermal [17], combustion [18], and sol–gel methods with several organic precursors [19–23]. Compared with other techniques, the sol–gel method is a useful and attractive technique for preparation of the $ZnAl_2O_4$ nanocrystals because of its advantage of producing pure and ultrafine powders at low temperatures. The starting materials used for the synthesis of Zinc aluminate spinel by the sol–gel methods employed by researchers were: $ZnCl_2$ and $AlCl_3$ hydrates with gelatin in H_2O [13], $Zn(NO_3)_2{\cdot}6H_2O$ and $Al(O^iPr)_3$ with nitric acid in ethyl alcohol [24], $Zn(NO_3)_2{\cdot}6H_2O$ and $Al(NO_3)_3{\cdot}9H_2O$ with citric acid in H_2O [25] and $Zn(NO_3)_2{\cdot}6H_2O$ and $Al(NO_3)_3{\cdot}9H_2O$ with triethanolamine and nitric acid in H_2O [26]. Wei and Chen have prepared nanosized zinc aluminate spinel by the thermal decomposition of Zn–Al gel prepared by sol–gel technique using oxalic acid as a chelating agent. The precursor on heating at 700 °C for 5 h yields single-phase $ZnAl_2O_4$ spinel [27]. Kurajica et al. [28] used of aluminum-*sec*-butoxide; $Al(O^sBu)_3$, and $Zn(NO_3)_2{\cdot}6H_2O$ as starting materials. Gels with and without chelating agent were prepared. Ethyl-acetoacetate was used as a chelating agent in order to control the rate of hydrolysis of $Al(O^sBu)_3$.

A modified sol–gel method for preparing the metal oxides is Pechini method [28]. The Pechini method involves combining a metal precursor with water, citric acid and a polyhydroxyalcohol, such as ethylene glycol [29–31]. In the present paper, $ZnAl_2O_4$ nanoparticles have been synthesized by modified Pechini method

* Corresponding author at: Institute of Nano Science and Nano Technology, University of Kashan, Kashan, P. O. Box. 87317-51167, I. R. Iran.
Tel.: +98 361 5555333; fax: +98 361 5552935.
** Corresponding author. Tel.: +98 361 5555333; fax: +98 361 5552935.
E-mail addresses: davar@kashanu.ac.ir (F. Davar), salavati@kashanu.ac.ir (M. Salavati-Niasari).

0925-8388/$ – see front matter © 2010 Elsevier B.V. All rights reserved.
doi:10.1016/j.jallcom.2010.11.058

Table 1
Comparison of particle size of the obtained $ZnAl_2O_4$ by different cconditions.

Sample	Precursor	Chelating agent	T (°C)/time (2 h)	Particle size (nm) (according to XRD results)	Products
1	$Zn(NO_3)_2 + Al(NO_3)_3$	Citric acid	450	–	ZnO (main) + $ZnAl_2O_4$ (minor)
2	$Zn(NO_3)_2 + Al(NO_3)_3$	Citric acid	550	23	$ZnAl_2O_4$ (main) + ZnO (minor)
3	$Zn(NO_3)_2 + Al(NO_3)_3$	Citric acid	600	25	$ZnAl_2O_4$
4	$Zn(NO_3)_2 + Al(NO_3)_3$	–	600	40	$ZnAl_2O_4$
5	$Zn(en)_2^{2+} + Al(NO_3)_3$	Citric acid	350	–	ZnO (main) + $ZnAl_2O_4$ (minor)
6	$Zn(en)_2^{2+} + Al(NO_3)_3$	Citric acid	450	20	$ZnAl_2O_4$ (main) + ZnO (minor)
7	$Zn(en)_2^{2+} + Al(NO_3)_3$	Citric acid	500	15	$ZnAl_2O_4$
8	$Zn(en)_2^{2+} + Al(NO_3)_3$	Citric acid	550	6	$ZnAl_2O_4$
9	$Zn(en)_2^{2+} + Al(NO_3)_3$	–	550	14	$ZnAl_2O_4$
10	$Zn(en)_2^{2+} + Al(NO_3)_3$	Citric acid	600	10	$ZnAl_2O_4$
11	$Zn(en)_2^{2+} + Al(NO_3)_3$	Citric acid	650	12	$ZnAl_2O_4$

using citric acid as a chelating agent, starting from aluminum nitrate and bis-ethylendiamine zinc (II), $Zn(en)_2^{2+}$ complex (en: ethylenediamine). The zinc atoms in the complex are tetrahedrally coordinated by two nitrogens from the ethylenediamine molecule. The alternating zinc and nitrogen atoms form five-member rings. These rings share edges to form layers that are perpendicular to the *a*-axis. Therefore, it can be anticipated that if one selects a suitable solvent that can extract or destroy ethylenediamine from the complex under mild conditions the zinc aluminium layers in the complex may be retained. In doing so, high-temperature $ZnAl_2O_4$ can be formed under mild and low-temperature conditions [32]. So this report is a simple, low temperature process with high crystalline and pure product. To the best of our knowledge, $Zn(en)_2^{2+}$ as a precursor for $ZnAl_2O_4$ nanoparticles synthesis is used for the first time. Characterization of the spinel powder was carried out by using X-ray diffraction (XRD), Fourier transform infrared spectroscopy (FTIR), scanning electron microscopy (SEM), and transmission electron microscopy (TEM).

2. Experimental

2.1. Materials and physical measurements

All the chemicals reagents used in our experiments were of analytical grade and were used as received without further purification. XRD patterns were recorded by a Rigaku D-max C III, X-ray diffractometer using Ni-filtered Cu Kα radiation. Scanning electron microscopy (SEM) images were obtained using Philips XL-30ESEM equipped with an energy dispersive X-ray spectroscopy. Transmission electron microscopy (TEM) images were obtained utilizing Philips EM208 transmission electron microscope with an accelerating voltage of 100 kV. Fourier transform infrared (FT-IR) spectra were recorded with Shimadzu Varian 4300 spectrophotometer in KBr pellets. Thermogravimetric analysis (TGA) were carried out using a thermal gravimetric analysis instrument (Shimadzu TGA-50H) with a flow rate of 20.0 mL min^{-1} and a heating rate of 10 °C min^{-1} in the air.

2.2. Synthesis of $Zn(en)_2^{2+}$ complex

To a stirred solution of $Zn(CH_3COO)_2{\cdot}2H_2O$ (1 mol) in ethanol, 2 mol of ethylenediamine was added. The reaction mixture was heated under reflux for 2 h and the solvent was removed under reduced pressure. The resulting yellow precipitate was collected and washed with deionized water and absolute ethanol to remove ions possibly remaining in the final product, and finally it was dried at 80 °C overnight in a vacuum oven. Anal. Calcd. (%) for $ZnN_4O_4H_{22}C_8$: C, 31.64; H, 7.30; N, 18.45; Zn, 21.53. Found (%): C, 31.68; H, 7.34; N, 18.47; Zn, 21.58.

2.3. Synthesis of $ZnAl_2O_4$ nanoparticles

At first 0.85 mmol of $Zn(en)_2^{2+}$ was dissolved in 10 ml diethylene glycol monoethyl ether (DGME) and 13.0 mmol of anhydrous citric acid ($C_6H_8O_7$) was subsequently added to this solution and heated at 60 °C for 2 h. Then 1.70 mol of $Al(NO_3)_3{\cdot}9H_2O$ in 8 ml diethylene glycol monoethyl ether was added. A dark yellow solution was obtained and further heated at 80 °C for 2 h to remove excess solvent. During continued heating at 120 °C for 1 h, the solution became more and more viscous and finally became a pale orange xerogel. For complete drying, xerogel was thermally treated at 230 °C for 1 h. Resultant yellow powder is as precursor. The precursor was further heat-treated at temperatures between 350 °C and 550 °C in air, in an Al_2O_3 furnace boat, and then cooled it to room temperature (Fig. 1 and Table 1). Two processes were adopted to prepare $ZnAl_2O_4$ nanoparticles, one process as summarized in Fig. 1 and another process was similar to Fig. 1 only the reaction was done without citric acid. Additionally, $ZnAl_2O_4$ samples were heated at higher temperatures to study their thermal stability.

Optimal condition for synthesizing $ZnAl_2O_4$ nanoparticles, (*sample 8*): 0.85 mmol of $Zn(en)_2^{2+}$ was dissolved in 10 ml DGME and 13.0 mmol of anhydrous citric acid was subsequently added to this solution and heated at 60 °C for 2 h. Then 1.70 mol of

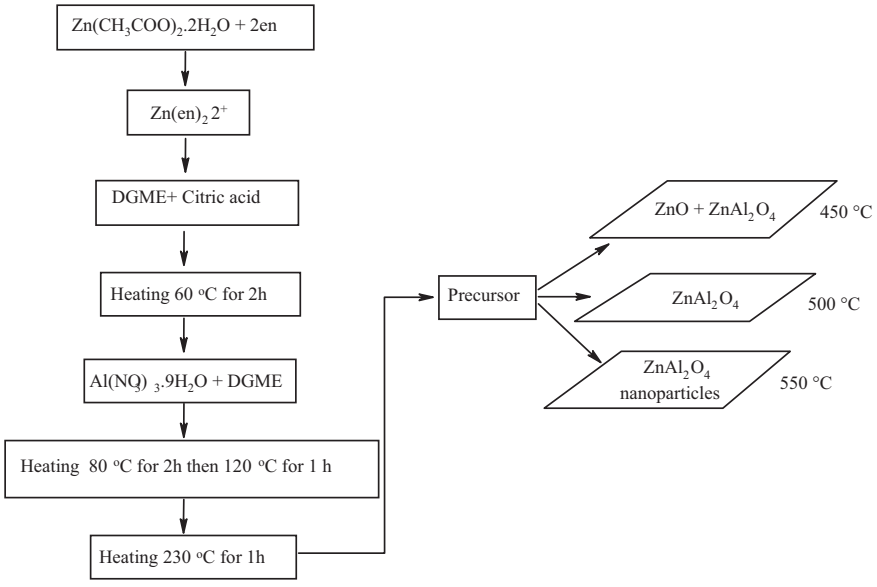

Fig. 1. Flow chart of $ZnAl_2O_4$ nanoparticles preparation procedure.

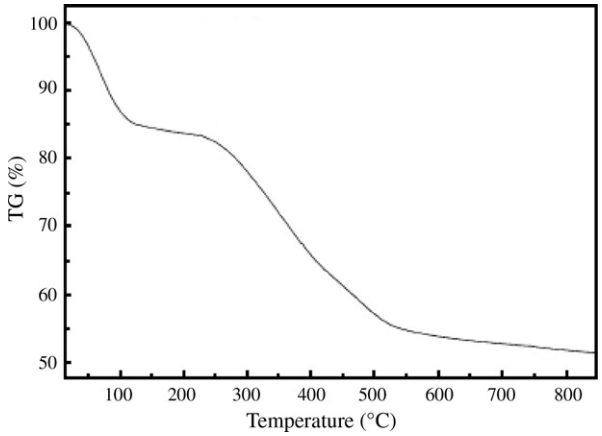

Fig. 2. Thermal gravimetric analyses curve of $ZnAl_2O_4$ precursor material prepared with the addition of citric acid.

$Al(NO_3)_3{\cdot}9H_2O$ in 8 ml DGME was added. The obtained solution was heated at 80 °C for 2 h to remove excess solvent and then continued heating at 120 °C for 1 h for preparing pale orange xerogel. For complete drying, xerogel was thermally treated at 230 °C for 1 h. The precursor was further heat-treated at 550 °C in air, in an Al_2O_3 furnace boat for 2 h, and then cooled to room temperature (Table 1).

3. Results and discussion

The stability of the precursor complex $Zn(en)_2^{2+}$ has investigated using the thermogravimetric (TG) analysis in the air. The TGA patterns of the as-synthesized precursor (Fig. 2) reveal weight loss steps between room temperature and ~100 °C and between 200 and 550 °C with an overall weight loss of 48.24%. The first weight loss step was attributed to the loss of adsorbed water, and the second weight loss was ascribed to decomposing of organic compound, structural water, N_2O_5 and CO_2.

No peak sequence that can be attributed either to zinc oxide or aluminum oxides or other impurity, could be found in the XRD pattern of the precursor. The effects of different treatment temperatures (350, 450, 500 and 550 °C) on the solid phase changes using $ZnAl_2O_4$ precursor are presented in Fig. 3a–d. In order to restrict crystallite growth, the calcination times at a fixed heating rate were carefully monitored to keep them as short as possible. It can be seen from the XRD patterns that $ZnAl_2O_4$ phase had not yet formed at 350 °C, indicating an a prevalence of amorphous phase and little amount of ZnO. With increasing annealing temperature, crystallization was occurred around 450 °C and the $ZnAl_2O_4$ phase was completely formed at 500 °C. The products annealed at 500 °C showed cubic $ZnAl_2O_4$ to be the only crystalline phase, and further increase of the annealing temperature to 550 °C resulted only with an increase of crystallinity of cubic $ZnAl_2O_4$ phase. The diffractograms of sample prepared with citric acid and without citric acid calcined at 550 °C as shown in Fig. 3d and e indicates that each sample is a monophasic spinel cubic (*Fd*3*m* with lattice size of 8.050 Å, JCPDS 73–1961). For two samples substantial crystallinity was achieved at 550 °C after calcination of the amorphous raw product for 2 h. However, crystallization was also possible at much lower temperatures. From XRD data Fig. 3d, the crystallite size (D_c) of the as-prepared $ZnAl_2O_4$ particles calcined at 550 °C for 2 h was calculated to be 6 nm using the Scherrer equation [33],

$$D_c = \frac{K\lambda}{\beta \cos\theta}$$

where β is the breadth of the observed diffraction line at its half-intensity maximum (3 1 1), K is the so-called shape factor, which usually takes a value of about 0.9, and λ is the wavelength of X-ray source used in XRD.

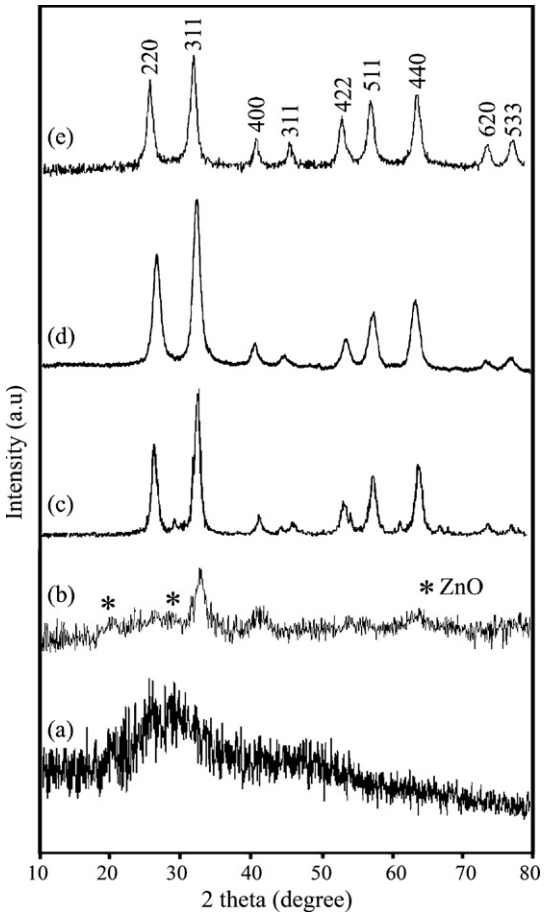

Fig. 3. XRD patterns of $ZnAl_2O_4$ powders obtained on heating the precursor in air for 2 h at (a) 350 °C, (b) 450 °C, (c) 500 °C, (d) 550 °C with citric acid and (e) 550 °C without citric acid.

The XRD pattern of the nanocrystals formed in the absence of citric acid shows a relatively sharp peak with higher intensity (Fig. 3e). When citric acid was introduced into the system, the organic ligand capped the nanocrystals surface, thereby inhibiting the growth of the particles. The XRD patterns of the nanocrystals modified with citric acid indicated that peaks intensities are smaller and the peak breadths are larger compared to unmodified samples (Fig. 3d). The average crystallite size of the unmodified nanocrystals calculated by the XRD data using Scheerer's equation is 14 nm, while the average crystallite size of nanocrystals synthesized with citric acid modification is about 6 nm.

The particle size of the obtained $ZnAl_2O_4$ nanoparticles was investigated by transmission electron microscopy (TEM) images. Fig. 4a and b shows the TEM images of prepared product in the presence of citric acid and without citric acid, respectively. TEM images indicate that $ZnAl_2O_4$ powders consists of nanometric particles, nanoparticles obtained from sample modified with citric acid were found to have slightly smaller particles with respect to unmodified sample, which is in good agreement with XRD. To investigate the size distribution of the nanoparticles particle size histograms were prepared for the $ZnAl_2O_4$ nanocrystals annealed at 550 °C (Fig. 4c and d). The information was obtained by measuring every nanoparticle on the TEM images of the same sample (80 nanoparticles). Most of the particles have 6 nm sizes for $ZnAl_2O_4$ modified with citric acid and 14 nm for the obtained products without citric acid.

It was found that nanocrystallinity of the modified sol–gel method-assisted heat treatment prepared $ZnAl_2O_4$ sample was retained after heating at 600 °C (sample 10); the average crystallite

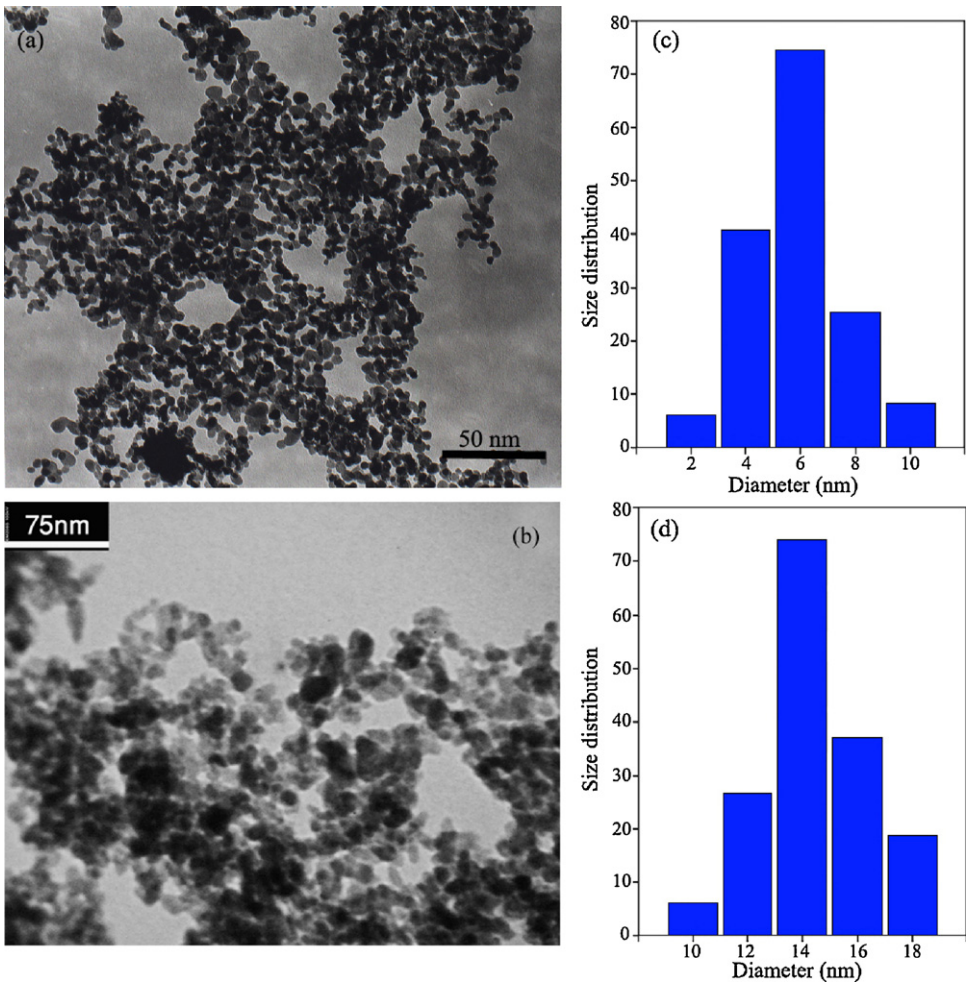

Fig. 4. (a, b) TEM images and (c, d) particle size histograms of $ZnAl_2O_4$ nanoparticles calcined at 550 °C modified with citric acid and without citric acid, respectively.

size increased slightly to ~10 nm. Fig. 5a and b shows TEM images of $ZnAL_2O_4$ nanoparticles calcined at 600 °C and 650 °C. As shown in Fig. 5, the crystallite size increases very slowly with increasing heating temperature. The average sizes of $ZnAl_2O_4$ nanoparticles heated in the 550 °C, 600 °C and 650 °C are found to vary from about 6, 10 and 15 nm. These results indicate good thermal stability of zinc aluminate obtained by this method. Similar results have been reported by using microwave-assisted solvothermal method [34] and hydrothermal methods with conventional heating [15] where much higher increase in the degree of crystallinity and in the crystallite size of zinc aluminate was observed after further heat treatment only at temperatures above 500 °C. It is notice that the nanostructured aluminates are of special interest due to their improved properties such as greater thermal stability and etc. [25].

Fig. 6 shows the infrared spectra of the precursor and the $ZnAl_2O_4$ system heat treated at 500 °C and 550 °C. Fig. 6a exhibits vibration bands corresponding to ethylenediamine molecules (above 3000 cm^{-1}, 2956, 2855, below 1200 cm cm^{-1}) [35]. In the IR spectra of $Zn(en)_2^{2+}$ precursor, the (υN–H) stretching vibration at frequencies above 3000 cm^{-1} all shift toward lower frequency compared with pure ethylenediamine, which might result from the chemical bonding action between Zn^{2+} and N atom. At frequencies below 1200 cm^{-1}, the IR spectra of the precursor exhibit many differences from the pure ethylenediamine, which should be due to the ordered alignment and regular conformation of ethylenediamine molecules in the precursor [36]. In these spectral vibrations (Fig. 6b and c) corresponding to the spinel structure are identified at about 490, 540 and 652 cm^{-1}. According to Dhak and Pramanik [26], the spinels display stretching bands in the 500–900 cm^{-1} range, associated with the vibrations of metal–oxygen, aluminum–oxygen and metal–oxygen–aluminum [36–38]. Bands around 490 cm^{-1}, 540 cm^{-1} and 652 cm^{-1} were found, and their intensity and area increased with increasing temperature (Fig. 6b and c). These bands correspond to the regular spinel structure with only sixfold coordinated aluminium [18], which is the only crystalline phase in accordance with the X-ray studies. These bands are ascribed to the Zn–O and Al–O vibrations related to tetrahedral [ZnO_4] and octahedral [AlO_6] groups [30] corresponding to regular spinel structure [19], which is the only crystalline phase in accordance with the X-ray studies.

There are two chemical reactions involved in the Pechini process: (i) chelation between complex cations and a hydroxycarboxylic acid (citric acid or EDTA etc.), (ii) polyesterification of excess hydroxycarboxylic acid with ethylene glycol [39]. Citric acid (CA) and ethylene glycol (EG) form a couple most widely employed in the Pechini process. CA can form very stable chelating complexes with many metal ions, and these formed metal–CA complexes can be further stabilized in EG as it possesses two alcoholic hydroxyl functional groups (–OH) with strong complexation affinities to metal ions, furthermore, two hydroxyl functional groups in one EG molecule can react with three carboxylic acid groups (–COOH) in one CA molecule to form a polyester resin. In this research diethylene glycol monoethyl ether (DGME) was applied instead of EG (see reported mechanism in Refs [40,41]). We pro-

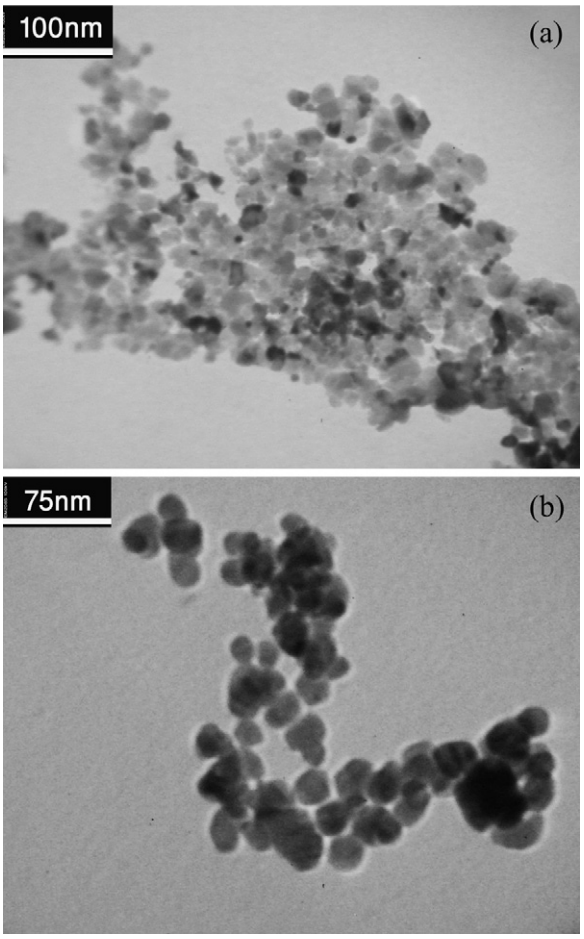

Fig. 5. TEM images of $ZnAl_2O_4$ nanoparticles calcined at (a) 600 °C, (sample 10) and (b) 650 °C, (sample 11).

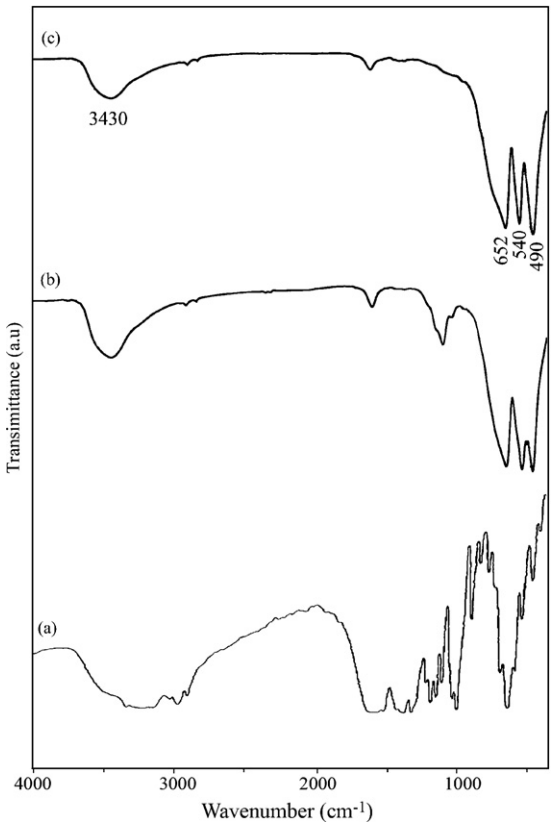

Fig. 6. FTIR spectra of (a) precursor powder, (b) after calcination of precursor powder for 2 h at 500 °C and (c) after calcination of precursor powder for 2 h at 550 °C.

posed the role of DGME be similar to EG. It is clear that glycol ethers, with the combination of ether, alcohol and hydrocarbon chain in one molecule, provide versatile solvency characteristics with both polar and non-polar properties. The effect of the pH on the formation of $ZnAL_2O_4$ can be interpreted in terms of different stability constant of Zn^{2+}–CA complex under different pH values. Citric acid is a tribasic acid that can be dissociated in aqueous solution to $C_6H_7O_7^-$, $C_6H_6O_7^{2-}$ and $C_6H_5O_7^{3-}$ depending on the pH of the solution. At low pH (pH ~2.0), $C_6H_7O_7^-$ is the prevailing species, which can interact with Zn^{2+} to form 1:1 complex $Zn(C_6H_7O_7)^+$ [39]. At high pH (pH ~6.0), $C_6H_5O_7^{3-}$ becomes the predominant species, which can interact more strongly with Zn^{2+} to form stable complex $Zn(C_6H_5O_7)^-$. According to stability constant for the above reaction, it is notice that the stability constant is high at large pH values, which implies the concentration of free Zn^{2+} in the solution decreasing and the homogeneity of Zn^{2+} and Al_2O_4 in the solution increasing, and also the homogeneity in the polyester precursor after the esterification is improved. The higher homogeneity promotes the formation of $ZnAl_2O_4$. The degree of chelation of metallic ions, by carboxylic groups (–COOH), in the starting solution is responsible for the uniformity of metallic constituents in the ester precursor after esterification. At higher pH conditions, more citric acid is ionized, more carboxylic group can be available to chelate the metallic ions in the solution, and higher uniformity of metal element in the ester can be attained [42]. The higher homogeneity promotes the formation of $ZnAl_2O_4$.

With reference to the results the citric acid as chelating-fuel agent was added to the solution. According to literature [43] citric acid has two different roles: to be a chelating agent for metallic ions and act as a fuel enabling the synthesis at relatively low temperatures. Here, citric acid as a chelating ligand coordinate to metallic ions, making the nucleation complete at the early stage of the so-gel process and inhibiting the crystal growth. In this time, metallic ions are capped completely with citric acid, so that, the Zn ions are protected against agglomeration, on the other hand, by increasing the citric acid molecules around the metal, we can obtain nanoparticles with the smallest size especially at lower calcination temperature. With reference to the above mentioned as-synthesized $ZnAl_2O_4$ nanoparticles in the presence of citric acid were smaller than obtained $ZnAl_2O_4$ nanoparticles without citric acid.

The choice of metal precursor is a key step in the production of metal oxides nanoparticles [44–48]. In addition, some other conditions were examined and compared with respect to the purity and particle size of the product, if any, and compare them with each other. According to Table 1 zinc nitrate and aluminum nitrate could be applied for preparation of $ZnAl_2O_4$, but when these precursors were used as a starting materials, the temperature of the goal product crystallization was higher, compared with the sample obtained using $Zn(en)_2^{2+}$. According to the Table 1 in the 550 °C, both ZnO and $ZnAl_2O_4$ were prepared. With increasing calcinations temperature to 600 °C, the X-ray data showed a complete conversion of the amorphous to the crystalline $ZnAl_2O_4$ phase at 600 °C. According to Table 1 and Fig. 3, when the $Zn(en)_2^{2+}$ was used as starting material, instead of zinc nitrate, $ZnAl_2O_4$ nanoparticles were synthesized successfully with the simplest conditions and the smallest size *via* calcinations of $Zn(en)_2^{2+}$ complex. The effect of precursor on the particle size of products could be for the steric hindrance, but the proposed mechanism for this observation need to other experimental.

4. Conclusion

In conclusion, the optimum condition for synthesizing $ZnAl_2O_4$ nanoparticles was investigated by modified sol–gel route. $ZnAl_2O_4$ nanoparticles were successfully synthesized through aluminum nitrate and $Zn(en)_2^{2+}$ complex (en: ethylenediamine) as new Zn^{2+} source. Diethylene glycol monoethyl ether and citric acid are employed as chelating ligand and solvent. However, our sol–gel experiments led to $ZnAl_2O_4$ below the decomposition temperature of the complex $Zn(en)_2^{2+}$. It appears that the solvent plays a crucial role in the formation of pure $ZnAl_2O_4$. The lowest temperature for preparation of the $ZnAl_2O_4$ nanocrystals is about 550 °C, which is not achieved when the material is prepared by more conventional methods. XRD measurements revealed no traces of impurities. The average crystallite size of the modified nanocrystals calculated by the XRD data was 6 nm. The results indicate also that $ZnAl_2O_4$ materials obtained under modified sol–gel conditions have a much better thermal stability as compared to $ZnAl_2O_4$ obtained through other methods.

Acknowledgement

Authors are grateful to council of University of Kashan for providing financial support to undertake this work.

References

[1] W.S. Tzing, W.H. Tuan, J. Mater. Sci. Lett. 15 (1996) 1395–1396.
[2] N. Bouropoulos, I. Tsiaoussis, P. Poulopoulos, P. Roditis, S. Baskoutas, Mater. Lett. 62 (2008) 3533–3535.
[3] R. Pandey, J.D. Gale, S.K. Sampath, J.M. Recio, J. Am. Ceram. Soc. 12 (1999) 3337–3341.
[4] J. Wrzyszcz, M. Zawadzki, J. Trawczynski, H. Grabowska, W. Mista, Appl. Catal. A 210 (2001) 263–269.
[5] S. Mathur, M. Veith, M. Haas, A. Shen, N. Lecerf, V. Huch, S. Hufner, R. Haberkorn, H.P. Beck, M. Jilavi, J. Am. Ceram. Soc. 84 (2001) 1921–1928.
[6] Y. Yang, X.W. Sun, B.K. Tay, J.X. Wang, Z.L. Dong, H.M. Fan, Adv. Mater. 19 (2007) 1839–1844.
[7] K. Kumar, K. Ramamoorthy, P.M. Koinkar, R. Chandramohan, K. Sankaranarayanan, J. Nanopart. Res. 9 (2007) 331–335.
[8] X. Gao, X. Li, W. Yu, J. Phys. Chem. B 109 (2005) 1155–1161.
[9] M. Salavati-Niasari, F. Davar, Mater. Lett. 63 (2009) 441–443.
[10] M. Salavati-Niasari, N. Mir, F. Davar, J. Alloys Compd. 476 (2009) 908–912.
[11] Y. Yang, D.S. Kim, R. Scholz, M. Knez, S.M. Lee, U. Gösele, M. Zacharias, Chem. Mater. 20 (2008) 3487–3494.
[12] W.-S. Hong, L.C. De Jonghe, X. Yang, M.N. Rahaman, J. Am. Ceram. Soc. 78 (1995) 3217–3224.
[13] N.J. van der Laag, M.D. Snel, P.C.M.M. Magusin, G. de With, J. Eur. Ceram. Soc. 24 (2004) 2417–2424.
[14] M.A. Valenzuela, J.P. Jacobs, P. Bosch, S. Reijne, B. Zapata, H.H. Brongersma, Appl. Catal. A: Gen 148 (1997) 315–324.
[15] M. Zawadzki, J. Wrzyszcz, Mater. Res. Bull. 35 (2000) 109–114.
[16] Z. Chen, E. Shi, Y. Zheng, W. Li, N. Wu, W. Zhong, Mater. Lett. 56 (2002) 601–605.
[17] M. Zawadzki, Solid State Sci. 8 (2006) 14–18.
[18] A.K. Adak, A. Pathak, P. Pramanik, J. Mater. Sci. Lett. 17 (1998) 559–561.
[19] N. Guilhaume, M. Primet, J. Chem. Soc. Faraday Trans. 90 (1994) 1541–1545.
[20] L.K. Kurihara, S.L. Suib, Chem. Mater. 5 (1993) 609–613.
[21] A.R. Phani, M. Passacantando, S. Santucci, Mater. Chem. Phys. 68 (2001) 66–71.
[22] Y. Wu, J. Du, K.-L. Choy, L.L. Hench, J. Guo, Thin Solid Films 472 (2005) 150–156.
[23] J.T. Keller, D.K. Agrawal, H.A. McKinstry, Adv. Ceram. Mater. 3 (1988) 420–422.
[24] X. Duan, D. Yuan, X. Wang, H. Xu, J. Sol–Gel Sci. Technol. 35 (2005) 221–224.
[25] X. Duan, D. Yuan, Z. Sun, C. Luan, D. Pan, D. Xu, M.K. Lv, J. Alloys Compd. 386 (2005) 311–314.
[26] D. Dhak, P. Pramanik, J. Am. Ceram. Soc. 89 (2006) 1014–1021.
[27] X. Wei, D. Chen, Mater. Lett. 60 (2006) 823–827.
[28] S. Kurajica, E. Tkalcec, J. Sipusic, G. Matijasic, I. Brnardic, I. Simcic, J. Sol–Gel Sci. Technol. 46 (2008) 152–160.
[29] M.P. Pechini, US 3,330,697 (1967).
[30] M. Salavati-Niasari, F. Davar, M. Farhadi, J. Sol–Gel Sci. Technol. 51 (2009) 48–52.
[31] M. Salavati-Niasari, M. Farhadi-Khouzani, F. Davar, J. Sol–Gel Sci. Technol. 52 (2009) 321–327.
[32] G.-T. Zhou, X. Wang, J.C. Yu, Crystal Growth Des. 5 (2005) 1761–1765.
[33] R. Jenkins, R.L. Snyder, Chemical Analysis: Introduction to X-ray Powder Diffractometry, John Wiley & Sons, Inc., New York, 1996, p. 90.
[34] M. Zawadzki, J. Alloys Compd. 439 (2007) 312–320.
[35] M. Salavati-Niasari, F. Davar, M.R. Loghman-Estarki, J. Alloys Compd. 494 (2010) 199–204.
[36] Z.X. Deng, C. Wang, X.M. Sun, Y.-D. Li, Inorg. Chem. 41 (2002) 869–873.
[37] K. Nakamoto, Infrared Spectra of Inorganic and Coordination Compound, 4th ed., Chemical Industry Press, Beijing, 1991.
[38] L.K.C. de Souza, J.R. Zamian, G.N. da Rocha Filho, L.E.B. Soledade, I.M.G. dos Santos, A.G. Souza, T. Scheller, R.S. Angélica, C.E.F. da Costa, Dyes Pigments 81 (2009) 187–192.
[39] Y. Xu, X. Yuan, G. Huang, H. Long, Mater. Chem. Phys. 90 (2005) 333–338.
[40] C. Sánchez, J. Doria, C. Paucar, M. Hernandez, A. Mósquera, J.E. Rodríguez, A. Gómez, E. Baca, O. Morán, Physica B 405 (2010) 3679–3684.
[41] S. Sakka, Handbook of Sol–Gel Science and Technology: Processing, Characterization and Application, Klumer Academic Publisher, Boston, London, 2005.
[42] Y. Xu, P. Lu, G. Huang, C. Zeng, Mater. Chem. Phys. 92 (2005) 220–224.
[43] A. Saberi, F. Golestani-Fard, H. Sarpoolaky, M. Willert-Porada, T. Gerdes, R. Simon, J. Alloys Compd. 142 (2008) 142–146.
[44] F. Davar, Z. Fereshteh, M. Salavati-Niasari, J. Alloys Compd. 476 (2009) 797–801.
[45] F. Davar, M. Salavati-Niasari, Z. Fereshteh, J. Alloys Compd. 496 (2010) 638–643.
[46] F. Mohandes, F. Davar, M. Salavati-Niasari, J. Magn. Magn. Mater. 322 (2010) 872–877.
[47] M. Salavati-Niasari, N. Mir, F. Davar, J. Alloys Compd. 493 (2010) 163–168.
[48] M. Salavati-Niasari, N. Mir, F. Davar, Appl. Surface Sci. 256 (2010) 4003–4008.